ELSEVIER SCIENCE Ltd. [DTD 4.1.0]
JOURNAL RMHM ARTICLE No. 2401
PAGES 1-6 DISPATCH 17 October 2000
RMHM 2401
PROD. TYPE: FROM DISK
A

International Journal of
REFRACTORY METALS
& HARD MATERIALS

ELSEVIER
International Journal of Refractory Metals & Hard Materials 000 (2000) 000–000

UNCORRECTED PROOF

Procedure development of laser welding of V–4Cr–4Ti alloy ☆

Zhiyue Xu *, Ken Natesan, Claude B. Reed, Dale L. Smith

Argonne National Laboratory, Building 308, 9700 South Cass Avenue, Argonne, IL 60439, USA

Received 16 February 2000; accepted 4 September 2000

Abstract

V–4Cr–4Ti alloy is selected as the structure material for the first wall/blanket in a fusion power reactor. A systematic study was conducted to develop a laser welding procedure for fabrication of vanadium alloy for the first wall/blanket systems. A 1.6 kW pulsed Nd:YAG laser with fiber optic beam delivery was used to carry out the bead-on-plate welding on 4 mm thick V–4Cr–4Ti plates. The process parameters, such as laser schedule power settings, beam travel speed, and welding atmosphere control, and their effects on weld quality, such as weld depth, porosity, and oxygen uptake were studied. Results from metallurgical characterization of the welds are presented. An innovative laser welding procedure has been developed to obtain deep penetration, defect free, and oxygen contamination free welds. © 2000 Elsevier Science Ltd. All rights reserved.

Keywords: Vanadium alloys; Laser welding; Procedure development; Bead-on-plate; Microhardness

1. Introduction

Vanadium alloy (V–4Cr–4Ti) is selected as the structure material for self-cooled lithium–vanadium blanket in a fusion reactor because of its accommodation of high heat loads, good mechanical properties at high temperatures, high neutron fluence capability, low degradation under neutron irradiation, good compatibility with the blanket materials, low decay heat, low waste disposal rating, and adequate strength to accommodate the electromagnetic loads during plasma disruption events [1,2]. Laser welding is considered as an attractive process in the construction of first wall/blanket system due to its high penetrating power and potential flexibility. Ideal laser welds are characterized by large weld depth, no weld defects, and small or no absorption of oxygen from the welding atmosphere. Large weld depth (larger than 3 mm) is required by the construction of the first wall/blanket and also by the preparation of the one-third-size Charpy impact test samples from the welds [3]. Weld defects and oxygen uptake should be avoided because they lead to embrittlement of the alloy. Early YAG laser welding tests on vanadium alloys in air with argon purge indicated that welds with weld depth close to 3 mm could be obtained but root porosity and oxygen uptake had always been the problem [4,5]. In this study, a systematic study was conducted to develop a laser welding procedure for fabrication of vanadium alloy for the first wall/blanket systems. Optimal laser schedule power settings were determined by laser parameter screening tests. Vanadium alloy is considered as a reactive metal because it reacts violently with atmospheric O_2 at elevated temperatures. Oxygen dissolves interstitially in vanadium and greatly decreases the ductility of the alloys [6]. Therefore, any welding performed on vanadium alloys must be performed in an environmental controlled atmosphere, or total inert atmosphere. For this reason, a custom-designed welding environmental control box (ECB) was integrated with the laser system to provide a controlled atmosphere for laser welding of vanadium alloy and protect it from oxidation. Weld depth, root porosity, microhardness cross weld width, and oxygen uptake were metallurgically characterized. As the result of current study, an innovative procedure has been de-

☆ The submitted manuscript has been created by the University of Chicago as Operator of Argonne National Laboratory ("Argonne") under contract No. W-31-109-ENG-38 with the U.S. Department of Energy. The U.S. Government retains for itself, and others acting on its behalf, a paid-up, nonexclusive, irrevocable worldwide license in said article to reproduce, prepare derivative works, distribute copies to the public, and perform publicly and display publicly, by or on behalf of the Government.

* Corresponding author. Tel.: +1-630-252-9172; fax: +1-630-252-6300.

E-mail address: zxu@anl.gov (Z. Xu).

0263-4368/00/$ - see front matter © 2000 Elsevier Science Ltd. All rights reserved.
PII: S 0 2 6 3 - 4 3 6 8 (0 0) 0 0 0 3 8 - X

veloped capable of producing deep penetration, defect free and oxygen contamination free welds.

2. Experimental procedures

The V–4Cr–4Ti alloy (500-kg Heat #832665) was selected for the study. The compositions and fabricating procedure of the vanadium alloy are reported elsewhere [3]. Bead-on-plate (BOP) welds were produced on 4-mm thick sheets of the alloy using a 1.6 kW pulsed YAG laser with fiber-optic beam delivery. The laser output power is dependent on the combination of laser schedule power settings, which include energy per unit time (E), pulse length (L), and pulse repetition rate (R). Screening tests for finding the optimal combination of laser schedule power settings were first conducted in air with a leading argon-gas purge at a flow rate of 25 l/s, provided by a 9.5-mm diameter tube at 30° from horizontal. Then welds were produced with optimal laser schedule power settings at different beam travel speeds. A custom-designed environmental control box (ECB) capable of purging with high-purity argon (99.995%) has been integrated with the YAG laser to improve the quality of the welding atmosphere. Fig. 1 schematically shows the set-up of the laser system with the ECB. The specimen was placed in the ECB with fixtures. The high-purity argon was purged into the box from both sides of the ECB at flow rate of 50 l/s for 30 s prior to welding to displace any air in the ECB. The flow rate was well controlled such that a slow flow of argon out from the slit on the top of the box could be formed. This provides a good welding atmosphere to minimize the oxygen uptake during the welding. A shielding disk just above the slit enhanced the shielding effect. An auxiliary side air knife was used to provide protection for the focussing lens from spatter and metal vapor contamination. The welds were sectioned transversely and longitudinally along the welds, and then metallurgically prepared for determining the weld depth and microhardness profile a cross the width of the weld, and comprehen-

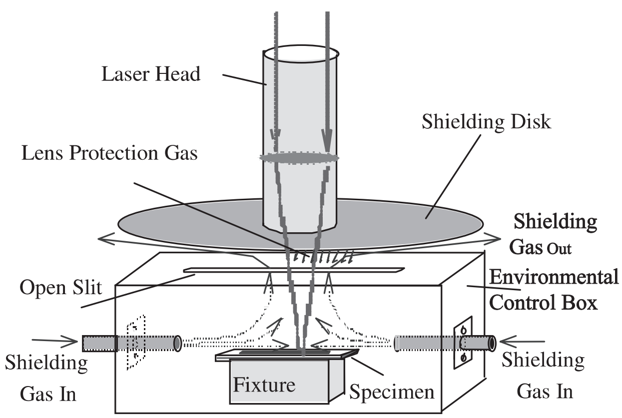

Fig. 1. Set-up of the laser welding system with welding environmental control box.

Table 1
Results of laser parameter screening tests

Test no.	Pulse settings $E/L/R$[a]	Beam travel speed (cm/s)	Focal lens	Weld depth (mm)	Spatter or humping?
1	6/2/132	1.5	5″	2.0	Y
2	6/2/132	2	5″	1.17	Y
3	5/2.5/128	1.5	5″	2.54	Y
4	5/2.5/128	2	5″	1.94	Y
5	4/3/132	0.5	5″	3.15	N
6	4/3/132	1	5″	2.81	N
7	4/3/132	1.5	5″	2.2	N
8	4/3/132	1.8	5″	2.17	N
9	4/3/132	2	5″	2.16	N
10	5.5/3/128	2.5	3″	2.5	Y
11	5.5/3/128	3	3″	1.92	Y
12	5/3/106	2	3″	2.5	Y
13	5/3/106	2.5	3″	2.43	Y
14	5/3/106	3	3″	1.79	Y
15	5.2/3/102	2	3″	2.8	Y
16	5.2/3/102	2.5	3″	2.37	Y
17	5.2/3/102	3	3″	2.1	Y
18	4/3/132	1	3″	3.8	N
19	4/3/132	1.5	3″	2.82	N
20	4/3/132	2	3″	2.8	N
21	4/3/132	3	3″	1.75	N
22	4/3/132	4	3″	1.66	N

[a] $E/L/R$ = pulse energy per unit time (J/ms)/pulse length (ms)/pulse repetition rate (Hz)

UNCORRECTED PROOF

sively examining for porosity. Vickers microhardness measurement a cross the weld width was accomplished using a Tukon Micro-Hardness Tester, Model-Mo. The applied load on the 136° diamond pyramid indenter was 500 g. The content of oxygen, nitrogen, and carbon of laser-welded samples produced with and without using the ECB were analyzed by inert gas fusion (IGF) method. The IGF samples are small chips (approximately 1×2 mm^2 in dimensions) milled from the core of the actual weld zone to guarantee the sample volume is over 99% made up by the weld zone.

3. Results and discussion

3.1. Laser parameter screening tests

The results of series of welds, produced at different combination of laser schedule power settings and beam travel speeds, are listed in Table 1. A 5″ or 3″ focussing lens was used to focus the beam at 1 mm into the specimen. Sound welds with large weld depth and no spatter or humping were obtained at pulse energy (E) of 4 J/ms, pulse length (L) of 3 ms, and pulse repetition rate (R) of 132 Hz at beam travel speed of 5 mm/s for 5″ lens and 10 mm/s for 3″ lens. Pulse energy larger than 4 J/ms generated welds with significant spatter and/or humping, which are the two major weld defects. Higher peak power as a result of higher E value in the laser schedule power settings disturbed the stabilization of the pressure in the weld pool and caused serious spatter and humping [7]. Laser pulse setting schedule, $E4/L3/R132$, was determined as the optimal laser parameters for the follow-up tests and beam travel speeds were adjusted for obtaining deep and porosity-free welds.

3.2. Porosity examination

Previously, root porosity was examined at a single, randomly selected cross-section via optical microscopy at 400×. Since the randomly chosen cross-section might be located at the no-porosity region just between the porosity, the porosity inspecting results from such cross-sections might give misleading information [4,5]. A comprehensive examination of the porosity should be conducted on the longitudinal sections along the centerline of the welds. Table 2 lists the welding conditions and weld depths of four example welds used to examine for porosity on longitudinal sections. The closeup of longitudinal section views of the welds are shown in Fig. 2. As revealed in Fig. 2, the number of porosity decreases as the beam travel speed decreases. Porosity-free

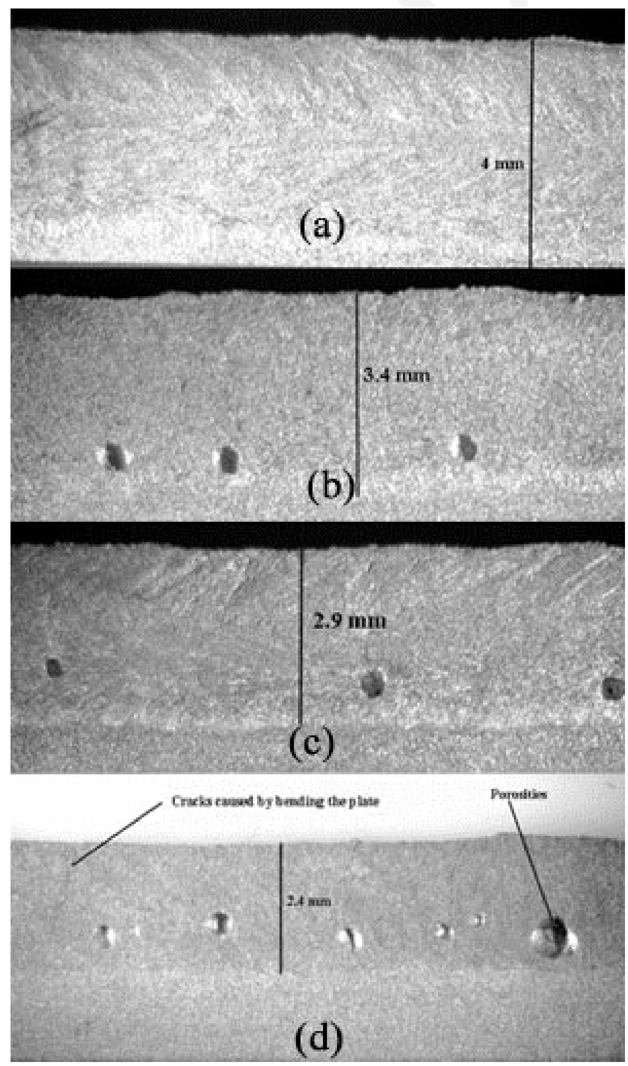

Fig. 2. Longitudinal section views of welds for comprehensive examination for porosity: (a) Weld No. 1, (b) Weld No. 2, (c) Weld No. 3, and (d) Weld No. 4.

Table 2
Welding conditions and weld depths for longitudinally sectioned samples

Weld No.	Laser energy (J/ms)	Pulse length (ms)	Repetition rate (Hz)	Beam travel speed (cm/s)	Weld depth (mm)
1	4	3	132	1	3.8
2	4	3	132	1.2	3.4
3	4	3	132	1.5	2.9
4	4	3	132	3.5	2.4

UNCORRECTED PROOF

UNCORRECTED PROOF

weld (Weld No. 1) was obtained when the weld depth reached the full thickness of the vanadium plate. It seems that full penetration provided a path on the bottom side of the vanadium plate for the gas trapped in the welding keyhole to escape, thus eliminating porosity.

3.3. Weld depth

Weld depth as a function of beam travel speed was determined for cross-sectioned and metallurgically prepared welds made with 3″ focussing lens at laser schedule power settings $E4/L3/R132$ via an optical microscopy (Fig. 3). Weld depth is of a first approximation inversely proportional to the beam travel speed for the given laser schedule power settings and focussing lens. Full penetration (3.8 mm) weld without drop-out was obtained at beam speed of 10 mm/s. Theoretically, any penetration between 3.8 and 1.32 mm can be achieved by using proper beam travel speed. There is no coupling of the laser beam with the material when the speed was larger than 50 mm/s.

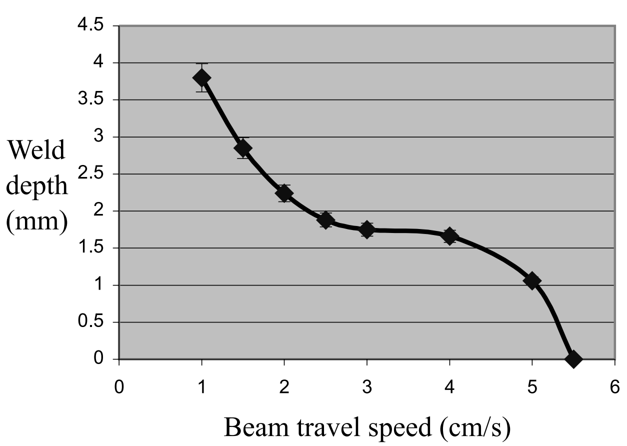

Fig. 3. Weld depth as a function of beam travel speed for a 3″ focussing lens and a given laser schedule power settings: energy per unit time of 4 J/ms, pulse length of 3 ms, and pulse repetition rate of 132 Hz.

3.4. Chemical analysis and microhardness evaluation

Concentrations of O, C, and N were analyzed by IGF method on the small chip samples milled directly from the actual weld zone produced at laser pulse setting schedule, $E4/L3/R132$, with or without using the environmental control box. The samples were wiped with acetone before and after welding except sample 990709B, which was cleaned in a pickling solution after welding. The results are compared in Table 3. Values for the reference heat (500-kg Heat # 832665) are also listed for information. The welds produced in the ECB with nearly optimal shielding gas (990712B and 990712C) have the lowest oxygen content (300 wppm). Welds using the ECB but with less than optimal shielding have higher oxygen content (360–390 wppm) compared to those with nearly optimal shielding. The welds obtained without using the ECB have the highest oxygen content (>1460 wppm). The O, N, and C contents of welds produced using the ECB with nearly optimal gas shielding are essentially the same as the reported values for the reference heat (310 wppm), indicating a successful protection of the weld from oxygen uptake during welding by the ECB design and shielding gas arrangement.

A microhardness profile across the width of weld 990712C is presented in Fig. 4. The profile shows some increase in hardness in the weld metal, in comparison to the adjacent base metal. The increase in hardness observed here (from ≈185 HV of base metal to ≈205 HV in weld zone) is in agreement with what was reported by Chung et al. [3]. A general trend of increasing microhardness with increasing oxygen content in weld metal was reported previously. It was considered that inter-

Table 3
IGF chemical analysis results of laser-welded V–Cr–Ti alloy samples

Sample	O (wppm)	C (wppm)	N (wppm)	Clean conditions before and after welding	Welded in environmental control box?
Heat 832665	310	80	85	Acetone wiped	Reference analysis
990223B	1460	60	1970	Acetone wiped	No
990223C	1690	80	2710	Acetone wiped	No
990709A	360	100	180	Acetone wiped	Yes, but non-optimal shielding gas flow
990709B	390	100	290	Cleaned in pickling solution after welding	Yes, but non-optimal shielding gas flow
990712B	320	100	70	Acetone wiped	Yes, near-optimal shielding gas flow
990712C	320	100	80	Acetone wiped	Yes, near-optimal shielding gas flow

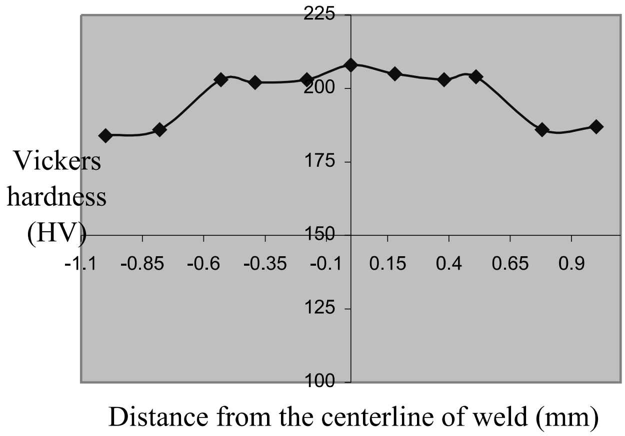

Fig. 4. Microhardness profile cross the width of a laser weld.

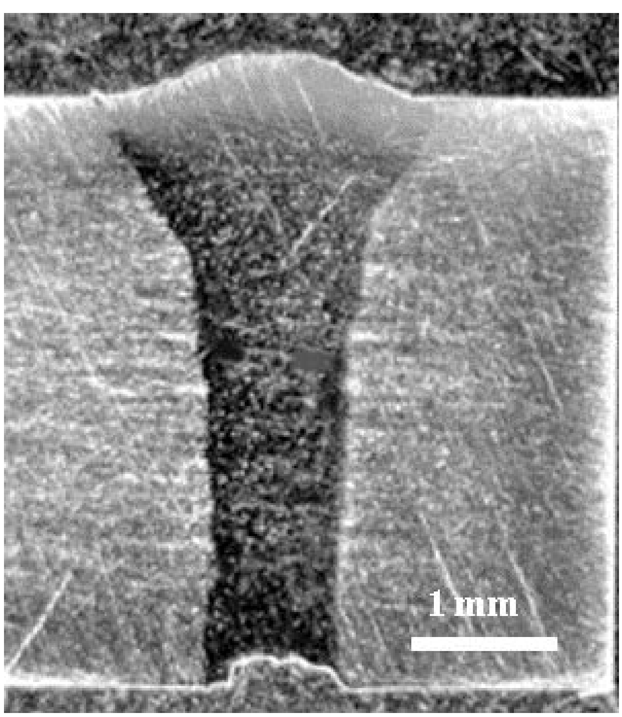

Fig. 5. Cross-section view of a fully-penetrated weld produced using the ECB with nearly optimal gas shielding, beam travel speed of 10 mm/s, and laser schedule power settings: energy per unit time of 4 J/ms, pulse length of 3 ms, and pulse repetition rate of 132 Hz.

stitial absorption of oxygen into the vanadium alloy lattice was the reason for the embrittlement of the alloy [8,9].

A cross-section metallography of a sound weld, produced using the ECB with nearly optimal shielding, beam travel speed of 10 mm/s and laser schedule power settings $E4/L3/R132$, is shown in Fig. 5. This fully penetrated weld has narrow width and does not reveal any cracks, porosity or other discontinuities. This indicates that high-quality joint is achieved with pulse YAG laser welding of vanadium alloy.

4. Conclusions

The following conclusions were made as a result of this procedure development of pulse YAG laser welding of vanadium alloy:

1. Optimal laser pulse parameters within the capabilities of the equipment for welding V–4Cr–4Ti alloy were determined as pulse energy of 4 J/ms, pulse length of 3 ms, and pulse repetition rate of 132 Hz.
2. Root porosity was eliminated for welds that have full penetration of the vanadium plates. Full penetration provided a path on the bottom side of the vanadium plate for the gas trapped in the weld to escape, thus eliminating porosity.
3. Weld depth is of a first approximation inversely proportional to the beam travel speed for the given laser schedule power settings and focussing lens. Full penetration (3.8 mm) weld without drop-out was obtained at beam speed of 10 mm/s, laser energy per unit time of 4 J/ms, pulse length of 3 ms, and pulse repetition rate of 132 Hz.
4. Oxygen uptake from the welding atmosphere can be significantly avoided by welding the material in a custom-designed environmental control box with nearly optimal shielding gas flow.

Acknowledgements

Work supported by the U.S. Department of Energy, Office of Fusion Energy, under Contract W031-109-Eng-38.

References

[1] Mattas RF, Loomis BA, Smith DL. Vanadium alloys for fusion application. JOM 1992;44(8):26.

[2] Loomis BA, Chung HM, Smith DL. Effect of neutron irradiation and hydrogen on ductile–brittle transition temperatures of V–Cr–Ti alloys. J Nucl Mater 1994;212–215:799–803.

[3] Chung HM, Park JH, Strain RV, Leong KH, Smith DL. Mechanical properties and microstructural charateristics of laser and electron-beam welds in V–4Cr–4Ti. J Nucl Mater 1998;258–263:1451–7.

[4] Natesan K, Smith DL, Xu Z, Leong KH. Laser-welded V–Cr–Ti alloys: microstructural and mechanical properties. Fusion Materials Semiannual Progress Report for Period Ending 30 June 1998, U. S. Department of Energy, Office of Fusion Energy Sciences, DOE/ER-0313/24, September 1998, pp. 87–90.

[5] Natesan K, Reed CB, Xu Z, Smith DL. Laser-welded V–Cr–Ti alloys: microstructural and mechanical properties. Fusion Materials Semiannual Progress Report for Period Ending 31 December

UNCORRECTED PROOF

1998, U. S. Department of Energy, Office of Fusion Energy Sciences, DOE/ER-0313/25, April 1999, pp. 64–68.

[6] Natesan K, Soppet WK. Effect of oxygen and oxidation on tensile behavior of V–5Cr–5Ti. Fusion Materials Semiannual Progress Report for Period Ending 31 January 1996, U. S. Department of Energy, Office of Fusion Energy Sciences, DOE/ER-0313/19, January 1996.

[7] Steen WM. Laser material processing. New York: Springer; 1991.

[8] Seybolt AU, Sumsion HT. Vanadium–Oxygen solid solutions. J Metals Trans AIME 1953;292–299.

[9] Fromm E, Gebhardt E. Gase und Kohlenstoff in Metallen. Berlin: Springer; 1976.

UNCORRECTED PROOF